$C_2H_5COOC_6H_5$ (5 mL), and toluene (14 mL). About 10% of C_2H_4 was consumed after the solution was stirred for 6 h. GLC analysis showed the formation of 1-butene.

Kinetic Studies. A 20-ml Schlenk tube containing $Ni(cod)_2$, ligand, aryl propionate, and solvent was connected to a vacuum line equipped with a mercury manometer and the system was evacuated. The Schlenk tube was surrounded by thermostated water controlled to ±0.5 °C. The reaction mixture was stirred by a magnetic stirrer and the rate of reaction was determined by measuring the volume of C_2H_4 evolved with time. When the concentration of ester was smaller than 0.5 M, the amount of C_2H_4 evolved became considerably smaller than 1 mol/$Ni(cod)_2$. This may be at least partly due to the trapping of the evolved C_2H_4 by nickel in the absence of enough of the ester and the data for the concentration range were omitted.

Spectral Measurement and Analysis. IR spectra were recorded on a Japan Electron Optics Laboratory (JEOL) Model JNM-PS-100 spectrometer, and ^{31}P NMR spectra on a JEOL Model JNM-PFT-PS-100 Fourier transform spectrometer. Microanalysis of C, H, and N was performed by Mr. T. Saito of our laboratory with a Yanagimoto CHN Autocorder Type MT-2. The analyses of gaseous and liquid products were carried out with a Shimadzu GC-3BT or GC-6A gas chromatograph.

References and Notes

(1) F. Dawans, J. C. Marechal, and P. Teyssie, *J. Organomet. Chem.*, **21**, 259 (1970).
(2) S. Komiya and A.Yamamoto, *J. Organomet. Chem.*, **87**, 333 (1970).
(3) G. P. Chiusoli, XXIIIrd International Congress of Pure and Applied Chemistry, Boston, 1971, Vol. 6, p 196.
(4) S. D. Ittel, C. A. Tolman, A. D. English, and J. P. Jesson, *J. Am. Chem. Soc.*, **100**, 7577 (1978).
(5) (a) T. Tatsumi, H. Tominaga, M. Hidai, and Y. Uchida, *Chem. Lett.*, 37 (1977); (b) M. Kubota, A. Miyashita, S. Komiya, and A. Yamamoto, Abstracts, 34th Annual Meeting of the Chemical Society of Japan, Hiratsuka, 1976, No. 3G05; (c) Y. Hashimoto, M. Mori, and Y. Ban, Abstracts, 26th Symposium on Organometallic Chemistry Japan, Kyoto, 1979, No. B206.
(6) (a) G. P. Chiusoli, G. Salerno, and F. Dallatomasina, *J. Chem. Soc., Chem. Commun.*, 793 (1977); (b) M. Catellani, G. P. Chiusoli, G. Salerno, and F. Dallatomasina, *J. Organomet. Chem.*, **146**, C19 (1978); (c) G. P. Chiusoli, G. Salerno, and F. Dallatomasina, *J. Chem. Soc., Chem. Commun.*, 793 (1977); (d) J. Tsuji, T. Yamakawa, M. Kaito, and T. Mandai, *Tetrahedron Lett.*, 2075 (1978); (e) B. M. Trost, *Tetrahedron*, **33**, 2615 (1977); (f) R. Baker, *Chem. Rev.*, **73**, 487 (1973).
(7) F. Dawans and P. Teyssie, *J. Polym. Sci., Part B*, **7**, 111 (1969).
(8) J. Ishizu, T. Yamamoto, and A. Yamamoto, *Chem. Lett.*, 1091 (1976).
(9) (a) H.-F. Klein and H. H. Karsch, *Chem. Ber.*, **109**, 2524 (1976); (b) S. Otsuka, A. Nakamura, T. Yoshida, M. Naruto, and K. Ataka, *J. Am. Chem. Soc.*, **95**, 3180 (1973); (c) T. Saruyama, T. Yamamoto, and A. Yamamoto, *Bull. Chem. Soc. Jpn.*, **49**, 546 (1976); (d) H.-F. Klein, *Angew. Chem.*, **85**, 403 (1973).
(10) (a) G. Wilke, German Patent 1 191 375 (1965); (b) G. Wilke, E. W. Muller, and M. Kröner, *Angew. Chem.*, **73**, 33 (1961); (c) F. Imaizumi, H. Ikeda, S. Hirayanagi, and K. Mori, *J. Chem. Soc. Jpn.*, 2205 (1975).
(11) (a) T. Nishiguchi, H. Imai, and K. Fukuzumi, *J. Catal.*, **39**, 375 (1975); (b) Y. Miura, J. Kiji, and J. Furukawa, *J. Mol. Catal.*, **1**, 447 (1976).
(12) T. Kohara, S. Komiya, T. Yamamoto, and A. Yamamoto, *Chem. Lett.*, 1513 (1979).
(13) T. Yamamoto, T. Saruyama, and A. Yamamoto, *Bull. Chem. Soc. Jpn.*, **49**, 589 (1976).
(14) T. Yamamoto, A. Yamamoto, and S. Ikeda, *J. Am. Chem. Soc.*, **93**, 3350 (1971).
(15) L. P. Hammett, "Physical Organic Chemistry", 2nd ed., McGraw-Hill, New York, 1970.
(16) (a) B. K. Morse and D. S. Tarbell, *J. Am. Chem. Soc.*, **74**, 416 (1952); (b) C. C. Price and W. J. Belanger, *ibid.*, **76**, 2682 (1954).
(17) T. Yamamoto, J. Ishizu, and A. Yamamoto, *Chem. Lett.*, 991, 1385 (1979).
(18) (a) J. Tsuji and K. Ohno, *Synthesis*, 157 (1969), and references cited therein; (b) M. C. Baird, C. J. Nyman, and G. Wilkinson, *J. Chem. Soc. A*, 348 (1968); (c) J. Tsuji, "Organic Synthesis by Means of Transition Metal Complexes", Springer-Verlag, West Berlin, 1975; (d) J. Blum, *Tetrahedron Lett.*, 1605, 3041 (1966); (e) G. A. Olah and P. Kreinenfuhl, *J. Org. Chem.*, **32**, 1614 (1967).
(19) (a) H. Goetz and S. Domin, *Justus Liebigs Ann. Chem.*, **704**, 1 (1967); (b) G. M. Kosolapoff and L. Maier, "Organic Phosphorus Compounds", Vol. 1, Wiley, New York, 1972, p 156.
(20) Y. Inoue, M. Hidai, and Y. Uchida, *Chem. Lett.*, 1119 (1972).
(21) P. W. Jolly and G. Wilke, "The Organic Chemistry of Nickel", Vol. I, Academic Press, New York, 1974.

The 147-nm Photolysis of Disilane[1]

G. G. A. Perkins and F. W. Lampe*

Contribution from the Davey Laboratory, Department of Chemistry, The Pennsylvania State University, University Park, Pennsylvania 16802.

Received August 30, 1979

Abstract: The photodecomposition of Si_2H_6 at 147 nm results in the formation of H_2, SiH_4, Si_3H_8, Si_4H_{10}, Si_5H_{12}, and a solid film of amorphous silicon hydride (a-Si:H). Three primary processes are proposed to account for the results, namely, (a) $Si_2H_6 + h\nu \rightarrow SiH_2 + SiH_3 + H$ ($\phi_a = 0.61$); (b) $Si_2H_6 + h\nu \rightarrow SiH_3SiH + 2H$ ($\phi_b = 0.18$); (c) $Si_2H_6 + h\nu \rightarrow Si_2H_5 + H$ ($\phi_c = 0.21$). The overall quantum yields depend on the pressure but at 1 Torr partial pressure of Si_2H_6 are $\Phi(-Si_2H_6) = 4.3 \pm 0.2$, $\Phi(SiH_4) = 1.2 \pm 0.4$, $\Phi(Si_3H_8) = 0.91 \pm 0.08$, $\Phi(Si_4H_{10}) = 0.62 \pm 0.03$, $\Phi(Si, wall) = 2.2$. Quantum yields for H_2 formation were not measured. A mechanism is proposed which is shown to be in accord with the experimental facts.

Introduction

A substantial amount of kinetic and mechanistic information concerning the gas-phase reactions of silicon hydride radicals has been gained through the photolysis and photosensitized decomposition of various silanes. Monovalent silyl radicals are known to undergo combination and disproportionation reactions[2-8] and are effectively intercepted by common free-radical scavengers such as nitric oxide[5,6] and olefins.[9,10] Divalent silylene radicals insert readily into Si–H bonds of the substrate molecule to yield higher silanes,[11-15] but are apparently less reactive toward olefins[16] and are unreactive toward nitric oxide.[13]

The direct photochemical decompositions of silane,[15] methylsilane,[12,13] and dimethylsilane[14] at 147 nm are characterized by the favored production of divalent silylene radicals in the primary step. The $Hg(^3P_1)$-photosensitized decompositions of monosilane,[4-7,9] disilane,[3] and the methylsilanes[5] occur predominantly through the formation and subsequent reaction of monovalent silyl radicals.

The direct photolysis of Si_2H_6 has not previously been reported. As part of a general research program concerned with the development of silicon hydride free-radical chemistry, we have studied the photodecomposition of Si_2H_6 at 147 nm. This paper is a report of our results.

Experimental Section

The photolyses were carried out in a 38-cm^3 cylindrical stainless steel cell fitted with a lithium fluoride window and coupled via a

0002-7863/80/1502-3764$01.00/0

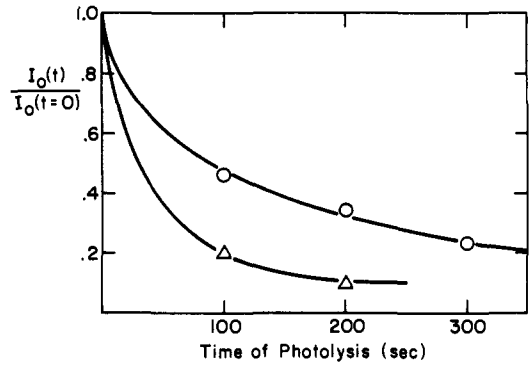

Figure 1. Reduction of incident light intensity by the formation of the film of amorphous silicon hydride on the window of the photolysis cell: ⊙, $P(SiH_4)$ = 1.9 Torr; △, $P(Si_2H_6)$ = 1.9 Torr.

Table I. Quantum Yields in the Photodecomposition of Si_2H_6 at 147 nm[a]

partial pressure Si_2H_6, Torr	$\Phi(-Si_2H_6)$	$\Phi(SiH_4)$	$\Phi(Si_3H_8)$	$\Phi(Si_4H_{10})$[b]
0.50	4.1 ± 0.3		0.68 ± 0.08	0.59 ± 0.06
0.95	4.3 ± 0.2			
1.00		1.2 ± 0.4	0.91 ± 0.08	0.62 ± 0.03
1.95	4.1 ± 0.4		1.18 ± 0.19	0.63 ± 0.04
4.36	4.1 ± 0.2		1.20 ± 0.08	0.54 ± 0.03

[a] Diluent gas = He; total pressure = 42 Torr. [b] This represents the total tetrasilane. We were unable to resolve the two isomers.

pinhole leak to a time-of-flight mass spectrometer. This apparatus and the xenon resonance lamp used as a light source have been described in a previous report.[15] The size of the pinhole leak was such that the average residence time of a stable molecule within the cell was 360 s. The reactant reservoirs were of such volume that during the course of an experiment the decrease in reactant pressure amounted to less than 2%.

The light intensity incident on the reactant mixture was determined by N_2O [$\Phi(-N_2O)$ = 1.7][18-21] and $(CF_3)_2CO$ [$\Phi(C_2F_6)$ from $(CF_3)_2CO$ = 1.11 at 4 Torr][22] actinometry. The intensity incident on the reaction mixture through a freshly cleaned window was 2.0 ± 0.2 × 10^{15} quanta/s.

The photodecomposition of silicon hydrides yields a solid deposit of amorphous silicon hydride on the walls and window of the photolysis cell. This results in the attenuation of incident intensity, as seen in Figure 1, in which the relative light intensity incident on $(CF_3)_2CO$ is plotted as a function of the time that the window has been exposed to SiH_4 and Si_2H_6 photodecomposition. The rate of solid deposition increases with pressure and is greater for Si_2H_6 than for SiH_4. Because of this time-dependent reduction in light intensity it was necessary to make actinometry measurements prior to each Si_2H_6 photolysis.

The photolyses were carried out with Si_2H_6 at partial pressures of 0.7–4 Torr. At these partial pressures of Si_2H_6 the light absorption is effectively complete. He was used as a diluting gas so that the total pressure in the cell was 40–50 Torr.

Si_2H_6 was made by the reduction of Si_2Cl_6 (Petrarch) with $LiAlH_4$ (Alfa Inorganics) using bis[2-(2-methoxyethoxy)ethyl] ether as solvent. When the gases formed in this reduction were separated on a vacuum line, it was found that the Si_2H_6 contained some SiH_3Cl impurity. This was effectively removed by letting the gases stand over a mixture of $LiAlH_4$ and $NaBH_4$ for a few days. Si_3H_8 and Si_4H_{10} were prepared from SiH_4 using the electric discharge method of Spanier and MacDiarmid.[23] SiH_4 was repeatedly passed through a glass ozonator, the higher silanes being condensed in a trap held at −131 °C (*n*-pentane slush bath). Si_2H_6 was first removed from the product mixture by raising the temperature of the mixture to −95 °C (toluene slush bath) and trapping the Si_2H_6 evolved at liquid-nitrogen temperature. Si_3H_8 was then isolated by holding the product mixture at −63 °C (chloroform slush bath) and trapping the volatile Si_3H_8 at liquid-nitrogen temperature. Finally Si_4H_{10} was isolated by holding the mixture at −29 °C (nitromethane slush bath) and trapping the volatile Si_4H_{10} at liquid-nitrogen temperature. Freeze–pump–thaw cycles from these slush baths were repeated several times to purify the Si_3H_8 and Si_4H_{10}. The mass spectra of pure Si_3H_8 and Si_4H_{10} taken before and after a final freeze–pump–thaw cycle were identical. The mass spectra of Si_3H_8 agreed well with the spectrum reported by Pupezin and Zmbov.[24] N_2O, NO, and high-purity He were purchased from the Matheson Co., Si_2D_6 was Merck Sharp and Dohme, and SiH_4 was from J. T. Baker. N_2O, Si_2D_6, and SiH_4 were subjected to a freeze–pump–thaw cycle before use. Nitric oxide was further purified by freezing onto a degassed silica gel trap at −195 °C followed by degassing at −195 °C. The frozen nitric oxide was then permitted to warm slowly and the middle 70% fraction was collected for use. He was used as received. All gas mixtures were prepared using a Saunders-Taylor apparatus.[25]

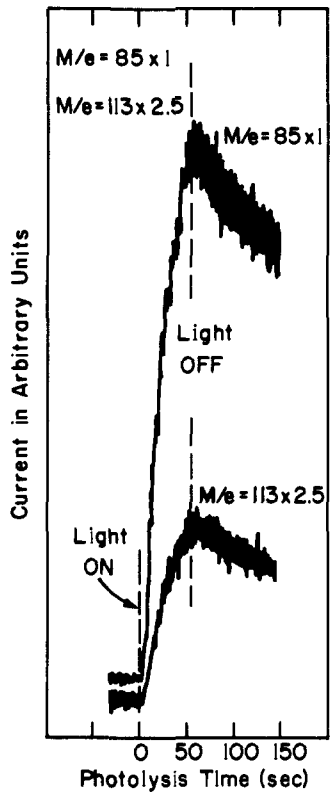

Figure 2. Formation of Si_3H_8 (m/e 85) and Si_4H_{10} (m/e 113) in the photolysis of Si_2H_6.

Results

The direct photolysis of Si_2H_6 at 147 nm results in the formation of H_2, SiH_4, Si_3H_8, Si_4H_{10}, Si_5H_{12}, and a solid deposit of amorphous silicon hydride on the walls and window of the photolysis cell. Si_3H_8 and Si_4H_{10} are both primary products. Figure 2 shows the ion currents of Si_3H^+ ($i_{85} \propto [Si_3H_8]$) and Si_4H^+ ($i_{113} \propto [Si_4H_{10}]$) and it may be seen here that Si_3H_8 and Si_4H_{10} are formed simultaneously with definite rates of production at the start of the photolysis. SiH_4, H_2, and the deposit of amorphous silicon hydride also show continuous production throughout the photolysis and are primary products. Trace amounts of Si_5H_{12} were detected; however, the amounts were just on the limit of our detector sensitivity.

1. Quantum Yields. Quantum yields for the formation of the volatile products and for the depletion of disilane are shown in Table I.

The quantum yields for the formation of Si_3H_8 and Si_4H_{10} were obtained from the initial slopes of i_{85} and i_{113}, respectively (cf. Figure 2), in photolyses carried out immediately after an actinometric measurement of the light intensity. The expressions[15] used to calculate the quantum yields are given as follows.

$$\Phi(Si_3H_8) = \frac{(di_{85}/dt)_0 V}{\beta_{85} I_{abs}} \quad (I)$$

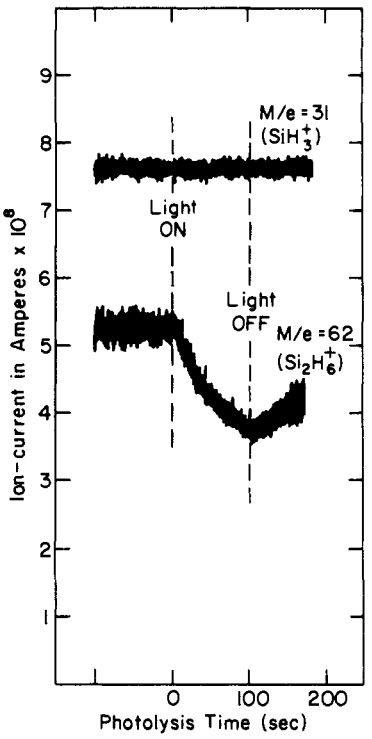

Figure 3. Formation of SiH_4 (m/e 31) and depletion of Si_2H_6 (m/e 62) in the photolysis of Si_2H_6.

$$\Phi(Si_4H_{10}) = \frac{(di_{113}/dt)_0 V}{\beta_{113} I_{abs}} \quad \text{(II)}$$

where β_{85} and β_{113} are mass spectrometric calibration factors relating ion currents at a given m/e to concentrations of the parent molecules. V is the volume of the photolysis cell, and I_{abs} is the light intensity absorbed by the Si_2H_6 in quanta/s. While the Beer's law extinction coefficient of Si_2H_6 at 147 nm is not known, one can estimate its value from the data[26] available on SiH_4 and SiH_3CH_3. At the partial pressures of Si_2H_6 employed and the geometry of our photolysis cell the absorption of incident light is essentially complete. Our method used to evaluate the incident light intensity has been discussed in previous reports.[15,22] Values of $\beta_{85}^{Si_3H_8}$ and $\beta_{113}^{Si_4H_{10}}$ were obtained by calibration of the mass spectrometer with known samples of Si_3H_8 and Si_4H_{10} mixed with He. In a photolysis the ion current at m/e 85 contains ions formed from the electron impact dissociation of Si_3H_8 and Si_4H_{10} and the rate expression $(di_{85}/dt)_0$ in (I) must be corrected for the contribution to i_{85} from Si_4H_{10}. This correction is easily made from the mass spectrum of pure Si_4H_{10} and the value of $(di_{113}/dt)_0$.

The quantum yield for the loss of Si_2H_6 was determined from the initial rate of depletion of Si_2H_6 ($i_{62} \propto [Si_2H_6]$) and the light intensity using the expression[15]

$$\Phi(-Si_2H_6) = -\frac{[Si_2H_6]_0 V}{i^0_{62} I_0}\left(\frac{di_{62}}{dt}\right)_0 \quad \text{(III)}$$

Expression III is similar to (I) and (II); i^0_{62} is the ion current of $Si_2H_6^+$ (m/e 62) before the photolysis is begun, $[Si_2H_6]_0$ is the initial concentration, and V is the volume of the photolysis cell. Note that the measurement of the initial rate of depletion of the reactant Si_2H_6 requires no prior calibration of the mass spectrometer. A typical recorder tracing, from which the initial slope $(di/dt)_0$ was calculated, is shown in Figure 3. A minor correction to $(di_{62}dt)_0$ is necessary owing to the contribution to m/e 62 from the electron impact dissociation of Si_3H_8. This correction, made from the mass spectra of pure Si_3H_8 and $(di_{85}/dt)_0$, amounts to less than 10%.

The quantum yield for the formation of SiH_4 was also evaluated in the experiments at 1 Torr pressure of Si_2H_6. In this case the ion current of SiH_3^+ (m/e 31) is a sum of contributions from SiH_4 and Si_3H_8 which are being produced and Si_2H_6 which is being depleted, as shown in the equation

$$(di_{31}^{measured}/dt)_0 = (di_{31}^{SiH_4}/dt)_0 + (di_{31}^{Si_2H_6}/dt)_0 + (di_{31}^{Si_3H_8}/dt)_0 \quad \text{(IV)}$$

where the first and third terms on the right-hand side are positive and the second term is negative. Upon substituting the relationship (V) into expression IV

$$(di_{31}^{X}/dt)_0 = \Phi_X I_0 \beta_{31}^{X} \quad \text{(V)}$$

and rearranging terms, one obtains the working equation (VI), viz.

$$\Phi_{SiH_4} = \left(\frac{di_{31}^{measured}}{dt}\right)_0 \frac{1}{I_0 \beta_{31}^{SiH_4}} + \Phi_{Si_2H_6}\frac{\beta_{31}^{Si_2H_6}}{\beta_{31}^{SiH_4}} - \Phi_{Si_3H_8}\frac{\beta_{31}^{Si_3H_8}}{\beta_{31}^{SiH_4}} \quad \text{(VI)}$$

which was used to calculate Φ_{SiH_4}. A typical recorder tracing from which $(di_{31}/di)_0$ was extracted is shown in Figure 3.

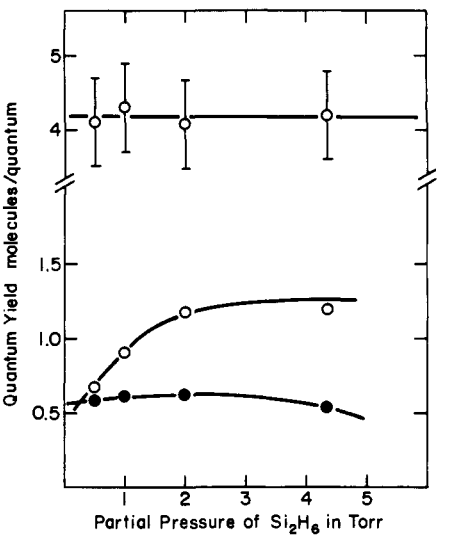

Figure 4. Dependence of quantum yields on the partial pressure of Si_2H_6: Φ, $\Phi(-Si_2H_6)$; ○, $\Phi(Si_3H_8)$; ●, $\Phi(Si_4H_{10})$.

The pressure dependence of the quantum yields for the decomposition of Si_2H_6 and the formation of Si_3H_8 and Si_4H_{10} is shown in Figure 4. These data are also given in Table I, where the quantum yield for the formation of monosilane is also shown. Each quantum yield listed is the mean of three to five replicate measurements and the uncertainties indicated are the average deviations from the mean. The larger uncertainties associated with $\Phi(-Si_2H_6)$ are due to the difficulty of accurately evaluating the initial slope, in the ion current at m/e 62, for the loss of Si_2H_6.

2. Effect of Nitric Oxide on Quantum Yields. From the quantum yields of the products in photolyses conducted in the presence of NO, it is possible to evaluate the quantum yields for the formation of various silylenes in the primary step.

Nitric oxide will react with the monovalent[3,5,6] silyl radicals to form siloxanes, but will not react with divalent silylene radicals.[13] Thus, in the presence of NO, only silylenes arising in the primary steps will react with Si_2H_6 to form higher silanes. Nitric oxide was added to the photolysis mixture at partial pressures such that its light absorption was negligible.

The quantum yields for the formation of Si_3H_8 and Si_4H_{10} in the photolysis of Si_2H_6 at a partial pressure of 0.6 Torr are shown in Figure 5. As the partial pressure of NO is increased larger fractions of monovalent silyl radicals are being inter-

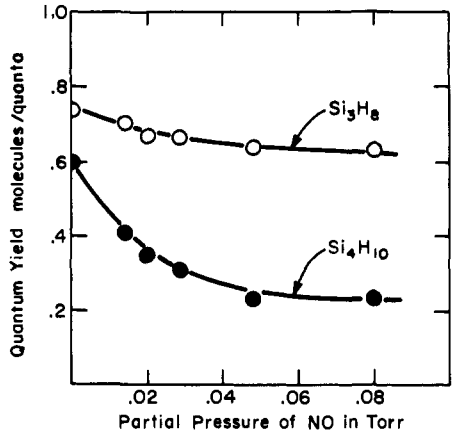

Figure 5. Dependence of $\Phi(Si_3H_8)$ and $\Phi(Si_4H_{10})$ on partial pressure of NO. Initial $P(Si_2H_6)$ = 0.6 Torr: ⊙, $\Phi(Si_3H_8)$; ●, $\Phi(Si_4H_{10})$.

cepted by NO, leading to the greater suppression of product quantum yields. The limiting values of $\Phi(Si_3H_8)$ and $\Phi(Si_4H_{10})$ under conditions of complete monovalent radical scavenging may be determined as the intercepts of plots of quantum yields vs. the reciprocal of NO partial pressures. Such plots are shown in Figure 6, from which it may be seen that $\Phi(Si_3H_8)$ is reduced by 17% and $\Phi(Si_4H_{10})$ by 70% of the values obtained in the absence of NO.

Discussion

1. Mechanism of the Photolysis. The results of the direct photolysis of Si_2H_6 at 147 nm are accounted for by the following reaction scheme:

$$Si_2H_6 + h\nu \rightarrow SiH_2 + SiH_3 + H \quad (a)$$

$$\rightarrow SiH_3SiH + 2H \quad (b)$$

$$\rightarrow Si_2H_5 + H \quad (c)$$

$$H + Si_2H_6 \rightarrow SiH_3 + SiH_4 \quad (1)$$

$$H + Si_2H_6 \rightarrow Si_2H_5 + H_2 \quad (2)$$

$$SiH_3 + Si_2H_5 \rightarrow Si_3H_8^* \quad (3)$$

$$Si_3H_8^* \rightarrow SiH_3SiH + SiH_4 \quad (4)$$

$$Si_3H_8^* + M \rightarrow Si_3H_8 + M \quad (5)$$

$$Si_2H_5 + Si_2H_5 \rightarrow Si_4H_{10}^* \quad (6)$$

$$Si_4H_{10}^* \rightarrow SiH_3SiH_2SiH + SiH_4 \quad (7)$$

$$Si_4H_{10}^* + M \rightarrow Si_4H_{10} + M \quad (8)$$

$$SiH_3 + SiH_3 \rightarrow Si_2H_6^* \quad (9)$$

$$Si_2H_6^* \rightarrow SiH_2 + SiH_4 \quad (10)$$

$$Si_2H_6^* \rightarrow SiH_3SiH + H_2 \quad (11)$$

$$Si_2H_6^* + M \rightarrow Si_2H_6 + M \quad (12)$$

$$SiH_3 + SiH_3 \rightarrow SiH_2 + SiH_4 \quad (13)$$

$$SiH_2 + Si_2H_6 \rightarrow Si_3H_8 \quad (14)$$

$$SiH_3SiH + Si_2H_6 \rightarrow Si_4H_{10} \quad (15)$$

$$SiH_3SiH_2SiH + Si_2H_6 \rightarrow Si_5H_{12} \quad (16)$$

$$SiH_3 + \text{wall} \rightarrow \text{solid} \quad (17)$$

$$Si_2H_5 + \text{wall} \rightarrow \text{solid} \quad (18)$$

The photochemical primary processes (a) and (b) that produce the singlet silylene species are necessary in order to account for the finite values of $\Phi(Si_3H_8)$ and $\Phi(Si_4H_{10})$ obtained under conditions of complete scavenging of monoradicals by NO. Thus Si_3H_8 is formed by the insertion of SiH_2 into the substrate Si_2H_6. Under conditions of complete interception of monoradicals, SiH_2 must be formed in a primary photochemical process and hence $\phi_a = 0.61$ (cf. Figure 6). Similarly, the formation of SiH_3SiH, which leads to the unscavenged production of Si_4H_{10}, occurs in primary process (b) with $\phi_b = 0.18$ (cf. Figure 6). In order to account for the fact that more than four molecules of Si_2H_6 are consumed per quantum absorbed (cf. Table I) it is necessary to postulate the formation of other reactive transients in primary processes (a) and (b) that can react with Si_2H_6. Within the limit fixed by the energy of a quantum of 147 nm (195 kcal/mol), the most likely additional reactive species formed are as shown in the reactions (a) and (b). Assuming that the total primary quantum yield is unity, we require at least one more primary process. This process must have a total quantum yield of 0.21 and yield products, namely, monoradicals, that are intercepted by NO. We have arbitrarily chosen this primary process, (c), to be a photodissociation to yield Si_2H_5 and H. A primary photodissociation to yield $2SiH_3$ radicals would equally well account for the results.

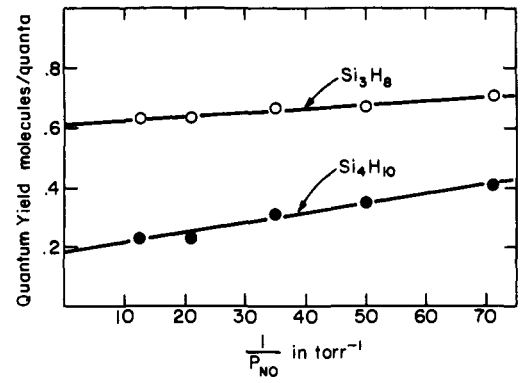

Figure 6. Extrapolation of quantum yields to conditions of complete monovalent-radical interception by NO. Initial $P(Si_2H_6)$ = 0.6 Torr.

Pollock, Sandhu, Jodhan, and Strausz[3] have shown that H atoms react with Si_2H_6 via (1) or (2) and that these reactions occur with a rate-constant ratio of $k_1/k_2 = 0.52$. The total rate constant for reaction of H atoms with Si_2H_6 is 3.7×10^{-12} cm^3/molecule·s,[3,27] a value sufficiently large to preclude the significant occurrence of any other reactions of H atoms under our conditions.

Reactions 3, 6, and 9 are the possible coupling reactions of monoradicals, while reactions 5, 8, and 12 represent the collisional deactivation of the vibrationally excited products of the radical coupling processes. The vibrationally excited molecules that are not collisionally stabilized will decompose to products of lower energy and the most likely such processes are the decompositions shown by reactions 4,[28] 7, 10,[8] and 11.[3]

It has been shown by Reimann, Matten, Laupert, and Potzinger[8] that reactions 9 and 13 occur with a rate-constant ratio at 300 K of $k_{13}/k_9 = 0.7$.

The chemically activated disilane molecule formed in reaction 9 contains an internal excitation energy of 73 kcal/mol and unless stabilized by the collisional process shown as reaction 12 will decompose. Decomposition via reaction 10 has been demonstrated by Reimann, Matten, Laupert, and Potzinger.[8] It was shown in our previous study[15] that the occurrence of reaction 11 was the most satisfactory explanation of the experimental results.

Finally, reactions 14–16 represent the insertion of singlet divalent silylene species into the Si–H bonds of the substrate, Si_2H_6. The ready occurrence of such reactions is well documented in the literature.[11]

The formation of the solid deposits of amorphous Si:H that

are observed on the walls and window of the reaction vessel is attributed to reactions of SiH_3 and Si_2H_5 at the wall, i.e., (17) and (18). No such deposit is observed in the absence of the light beam and the presence of small amounts of NO significantly reduces the formation rate of this deposit and, therefore, it seems most probable that reactions of the monoradicals SiH_3 and Si_2H_5 at the vessel surfaces are responsible for the formation of amorphous Si:H. This conclusion is in accord with available kinetic data which indicate that, of the reactive species produced by light absorption, only SiH_3 and Si_2H_5 are sufficiently unreactive toward Si_2H_6 to reach the walls of the vessel. From a material balance on silicon-containing species in the photolysis at 1.00 Torr partial pressure of Si_2H_6, it is possible to derive a quantum yield for Si atoms going to amorphous Si:H of $\phi(\text{Si, surface}) = 2.2$. Another way of stating this fact is that, at 1 Torr partial pressure of Si_2H_6, the products SiH_4, Si_3H_8, and Si_4H_{10} account for 75% of the disilane that has reacted. Although yields of SiH_4 were not measured for other partial pressures of Si_2H_6, the yields of Si_3H_8 and Si_4H_{10} suggest that at higher partial pressures of reactant the material balance increases above 75%. A similar dependence of the material balance on reactant partial pressure was observed in the study of SiH_4 photodecomposition.[15] As in that previous study,[15] we assume here that above 1 Torr partial pressure of reactant it is a reasonable approximation to neglect the surface reactions of SiH_3 and Si_2H_5 in a kinetic treatment of the mechanism.

2. Kinetic Treatment of the Mechanism. Although the mechanism is complex, a fortuitous distribution of the primary quantum yields, ϕ_a, ϕ_b, and ϕ_c, coupled with the branching ratio[3] (k_1/k_2), permits a simplifying approximation to be made. The only reactions in which SiH_3 and Si_2H_5 are consumed are the radical–radical encounters (3), (6), (9), and (13). According to the usual simple kinetic theory approximation for molecular encounters, namely, $k_3 = 2k_6 = 2(k_9 + k_{13})$, one may assume that SiH_3 and Si_2H_5 radicals are consumed approximately at the same rate.

Using the steady-state approximation for H atoms it is easy to show from the mechanism proposed that the ratio of rates of formation of SiH_3 and Si_2H_5 radicals is

$$\frac{d[SiH_3]/dt}{d[Si_2H_5]/dt} = \frac{\phi_a + (\phi_a + 2\phi_b + \phi_c)/(1 + (k_2/k_1))}{\phi_c + (\phi_a + 2\phi_b + \phi_c)/(1 + (k_1/k_2))} \quad \text{(VII)}$$

Substitution of the observed primary quantum yields, namely, $\phi_a = 0.61$, $\phi_b = 0.18$, $\phi_c = 0.21$, and the branching ratio $(k_1/k_2) = 0.52$[3] into (VII) yields the value 1.03. Therefore, within an error of 3% the mechanism predicts that the rates of formation of SiH_3 and Si_2H_5 are equal. Since, within the limits of simple kinetic theory, the loss rates are equal, we may make the approximation that $[SiH_3] = [Si_2H_5]$.

A standard steady-state kinetic treatment of the mechanism using the above approximation yields the expressions shown in (VIII)–(X) for the quantum yields.

$$\Phi(Si_3H_8) = \phi_a + \frac{\phi_a + \left(\frac{k_1}{k_1 + k_2}\right)(\phi_a + 2\phi_b + \phi_c)}{4(k_9 + k_{13})} \times \left(k_{13} + \frac{k_9 k_{10}}{k_{10} + k_{11} + k_{12}[M]}\right) + \frac{1}{2}\frac{\sqrt{\alpha + \beta(k_2/k_1) + \gamma(k_2/k_1)^2}}{1 + (k_2/k_1)}\frac{k_5[M]}{k_4 + k_5[M]} \quad \text{(VIII)}$$

$$\Phi(Si_4H_{10}) = \phi_b + \frac{1}{2}\frac{\sqrt{\alpha + \beta(k_2/k_1) + \gamma(k_2/k_1)^2}}{1 + (k_2/k_1)} \times \left(\frac{k_4}{k_4 + k_5[M]}\right) + \frac{k_8[M]}{k_7 + k_8[M]}\left(\frac{\phi_c + \left(\frac{k_2}{k_1 + k_2}\right)(\phi_a + 2\phi_b + \phi_c)}{4}\right) + \frac{1}{4}\frac{k_{11}}{k_{10} + k_{11} + k_{12}[M]} \times \left(\frac{\phi_a + \left(\frac{k_1}{k_1 + k_2}\right)(\phi_a + 2\phi_b + \phi_c)}{1 + k_{13}/k_9}\right) \quad \text{(IX)}$$

$$\Phi(-Si_2H_6) = 3 + \frac{1}{4}\frac{\phi_a + \left(\frac{k_1}{k_1 + k_2}\right)(\phi_a + 2\phi_b + \phi_c)}{(k_9 + k_{13})} \times \left(k_{13} + \frac{k_9(k_{10} + k_{11})}{k_{10} + k_{11} + k_{12}[M]}\right) + \frac{1}{2}\frac{\sqrt{\alpha + \beta(k_2/k_1) + \gamma(k_2/k_1)^2}}{1 + k_2/k_1}\left(\frac{k_4}{k_4 + k_5[M]}\right) - \frac{1}{4}\frac{k_{12}[M]}{k_{10} + k_{11} + k_{12}[M]} \times \left(\frac{\phi_a + \left(\frac{k_1}{k_1 + k_2}\right)(\phi_a + 2\phi_b + \phi_c)}{1 + k_{13}/k_9}\right) \quad \text{(X)}$$

In (VIII)–(X), α, β, and γ are functions of the primary quantum yields. Specifically

$$\alpha = \phi_c^2 + 2\phi_a\phi_c + 2\phi_b\phi_c$$

$$\beta = 2(\phi_a^2 + 2\phi_b^2 + \phi_c^2 + 3\phi_a\phi_b + 3\phi_a\phi_c + 3\phi_b\phi_c)$$

$$\gamma = \phi_c^2 + 2\phi_a\phi_b + 2\phi_a\phi_c$$

Substitution of the experimental values for the primary quantum yields and the value of the ratio $k_{13}/k_9 = 0.7$[8] into (VIII) yields the expression

$$\Phi(Si_3H_8) = 0.71 + \frac{0.15k_{10}}{k_{10} + k_{11} + k_{12}[M]} + 0.46\frac{k_5[M]}{k_4 + k_5[M]} \quad \text{(XI)}$$

The results of our previous study,[15] coupled with that of Reimann, Matten, Laupert, and Potzinger,[8] suggest that $k_{10} \ll k_{11}$ and therefore the second term on the right side of (XI) is negligible. It is thus seen that (XI) predicts the correct form of the pressure dependence of $\Phi(Si_3H_8)$ and that the high-pressure limiting value of $\Phi(Si_3H_8) = 1.17$ is in excellent agreement with the experimental results (cf. Figure 4).

Similarly, substitution of the experimental values of the primary quantum yields into (IX) yields the expression

$$\Phi(Si_4H_{10}) = 0.18 + 0.46\frac{k_4}{k_4 + k_5[M]} + 0.25\frac{k_8[M]}{k_7 + k_8[M]} + \frac{0.15k_{11}}{k_{10} + k_{11} + k_{12}[M]} \quad \text{(XII)}$$

At 1 Torr partial pressure and above, the previous results[8,15] suggest that $k_{11} \gg k_{10} + k_{12}[M]$. Therefore (XII) predicts a pressure dependence that is consistent with the experimental data and a high-pressure limit, $\Phi(Si_4H_{10}) = 0.58$, that is in good agreement with the results shown in Figure 4.

Substitution of the primary quantum yields into (X) yields an expression that predicts that $\Phi(-Si_2H_6)$ should be a slowly decreasing function of the partial pressure of Si_2H_6. This form is consistent with the data in Figure 4, although the low-pressure value of $\Phi(-Si_2H_6) = 3.6$ predicted by (X) is somewhat lower than the values observed. Possibly reactions of Si_2H_6 at

active surfaces, processes not accounted for in the mechanism, are responsible for the additional depletion of Si_2H_6.

Considering the complexity of the reaction and the approximations used in the kinetic treatment we consider (VIII)–(X) to be satisfactory representations of the experimental results. Since they were derived from the mechanism proposed, the extent of the agreement with the experiment provides a measure of the validity of the mechanism in describing the photochemical decomposition of Si_2H_6. It is admittedly only a partial mechanism because it does not in any way account for the formation of the solid deposit of amorphous Si:H.

3. Formation of Solid. The solid deposit must be formed by reaction of silicon-containing intermediates at the walls and window of the photolysis cell. The rate constant of (14) is known to be so large (i.e., 6.15×10^{-12} cm^3/molecule·s)[29] that under our conditions SiH_2 molecules will not reach the walls in significant amounts before they react in the gas phase. By analogy we assume that this is also true for the other silylene species SiH_3SiH and SiH_3SiH_2SiH. This leaves the monoradicals SiH_3 and Si_2H_5 as the only silicon-containing transients that can be responsible for the buildup of solid. This conclusion is consistent with those reached in earlier studies of the H-atom-induced decomposition of silanes[30] and of the 147-nm photolysis of SiH_4.[15] It is also in accord with the fact that the presence of NO inhibits significantly the formation of the solid deposits.

Acknowledgment. This work was supported by the U.S. Department of Energy under Contract EY-76-S-02-3416.

References and Notes

(1) U.S. Department of Energy Document No. EY-76-S-02-3416-12.
(2) Ring, M. A.; Beverly, G. D.; Koester, F. H.; Hollandsworth, R. P. *Inorg. Chem.* **1969**, *8*, 2033.
(3) Pollock, T. L.; Sandhu, H. S.: Jodhan, A.; Strausz, O. P. *J. Am. Chem. Soc.* **1973**, *95*, 1017.
(4) Niki, H.; Mains, G. J. *J. Phys. Chem.* **1964** *68*, 304.
(5) Nay, M. S.; Woodall, G. N. C.; Strausz, O. P.; Gunning, H. E. *J. Am. Chem. Soc.* **1965**, *87*, 179.
(6) Kamaratos, E.; Lampe, F. W. *J. Phys. Chem.* **1970**, *74*, 2267.
(7) Austin, E. R.; Lampe, F. W. *J. Phys. Chem.* **1976**, *80*, 2811.
(8) Reimann, B.; Matten, A.; Laupert, R.; Potzinger, P. *Ber. Bunsenges. Phys. Chem.* **1977**, *81*, 500.
(9) White, D.; Rochow, E. G. *J. Am. Chem. Soc.* **1954**, *76*, 3987.
(10) Schmidt, J. F.; Lampe, F. W. *J. Phys. Chem.* **1969**, *73*, 2706.
(11) Gaspar, P. P. In "Reactive Intermediates", Jones, Jr., M., Moses, R. A., Eds.; Wiley: New York, 1978; p 245 ff, and references cited therein.
(12) Strausz, O. P.; Obi, K.; Duholke, W. K. *J. Am. Chem. Soc.* **1968**, *90*, 1359.
(13) Obi, K.; Clement, A.; Gunning, H. E.; Strausz, O. P. *J. Am. Chem. Soc.* **1969**, *91*, 1622.
(14) Alexander, A. G.; Strausz, O. P. *J. Phys. Chem.* **1976**, *80*, 2531.
(15) Perkins, G. G. A.; Austin, E. R.; Lampe, F. W. *J. Am. Chem. Soc.* **1979**, *101*, 1109.
(16) Atwell, W. H.; Weyenberg, D. R. *J. Am. Chem. Soc.* **1968**, *90*, 3438.
(17) Gorden, R.; Rebbert, R. E.; Ausloos, P. *Natl. Bur. Stand. (U.S.), Tech. Note* **1969**, *No. 496*.
(18) Zelikoff, M.; Aschenbrand, L. M. A. *J. Chem. Phys.* **1954**, *22*, 1680.
(19) Groth, W. E.; Schlerholz. *Planet. Space Sci.* **1959**, *1*, 333.
(20) Yang, J. Y.; Servedio. F. M. *J. Chem. Phys.* **1967**, *47*, 4817.
(21) Dodge, M. C.; Heicklen, J. P. *Int. J. Chem. Kinet.* **1971**, *3*, 269.
(22) Perkins, G. G. A.; Austin, E. R.; Lampe, F. W. *J. Chem. Phys.* **1978**, *68*, 4357.
(23) Spanier, E. J.; MacDiarmid, A. G. *Inorg. Chem.* **1962**, *1*, 432.
(24) Pupezin, J. D.; Zmbov, K. F. *Bull. Inst. Nucl. Sci. "Boris Kidrich"* **1958**, *8*, 89.
(25) Saunders, K. W.; Taylor, H. A. *J. Chem. Phys.* **1941**, *9*, 616.
(26) Harada, Y.; Murrel, J. N.; Sheena, H. H. *Chem. Phys. Lett.* **1968**, *1*, 595.
(27) Austin, E. R.; Lampe, F. W. *J. Phys. Chem.* **1977**, *81*, 1134.
(28) Sefcik, M. D.; Ring, M. A. *J. Am. Chem. Soc.* **1973**, *95*, 5168.
(29) John, P.; Purnell, J. H. *J. Chem. Soc., Faraday Trans. 1* **1973**, *69*, 1455.
(30) Austin, E. R.; Lampe, F. W. *J. Phys. Chem.* **1977**, *81*, 1134.

Metal–Silicon Bonded Compounds. 12. Crystal and Molecular Structure of Hexameric Trimethylsilyllithium, $[LiSiMe_3]_6$

William H. Ilsley, Theodore F. Schaaf, Milton D. Glick, and John P. Oliver*

Contribution from the Department of Chemistry, Wayne State University, Detroit, Michigan 48202. *Received August 4, 1977*

Abstract: The crystal and molecular structure of hexameric trimethylsilyllithium is reported. The structure has been determined from single-crystal X-ray data collected by counter methods and solved by application of the Sayre relationship. Crystals of trimethylsilyllithium are monoclinic with space group $P2_1/a$ with $Z = 4$ and cell dimensions of $a = 13.933$ (3) Å, $b = 14.078$ (3) Å, $c = 18.902$ (4) Å, and $\beta = 89.60$ (2)°. Full-matrix least-squares refinement gave final discrepancy factors of $R_1 = 0.042$ and $R_2 = 0.047$ for 1563 data having $I > 3\sigma(I)$. The molecular structure consists of discrete centrosymmetric hexameric units with a core of lithium atoms surrounded by trimethylsilyl groups. The geometry of the lithium core can be described in terms of a six-membered ring in a highly folded chair conformation with an acute seat-to-back angle or, alternatively, as a distorted octahedron severely compressed along a threefold axis so as to form a shortened trigonal antiprism. The six side triangular faces of the antiprism each have one long (3.25 (4) Å) and two short (2.72 (2) Å) Li–Li distances. The trimethylsilyl groups lie above these sides and are somewhat more closely associated with the two lithium atoms related by the longest lithium–lithium distance. The two average lithium–silicon distances are 2.65 and 2.77 Å. The bonding is described in terms of four-centered electron-deficient Si–Li bonds with minimal Li–Li or Li–H interactions.

Introduction

The structures of electron-deficient organometallic compounds are of continuing interest because of their unusual bonding and reactivity. The most complex of these species (excluding those of boron) are represented by the oligomeric derivatives of alkyllithium compounds. Much of the early work with regard to both the structure of and bonding in these molecules has been discussed by Brown[1] and recent structural studies have been reviewed by Oliver.[2] Only a limited number of studies have appeared which deal quantitatively with the structures of the simple organolithium species and of the related metalates. These studies include the determination of the crystal structures of methyllithium,[3,4] ethyllithium,[5] cyclohexyllithium,[6] and bicyclo[1.1.0]butan-1-yllithium–TMEDA.[7]

0002-7863/80/1502-3769$01.00/0